

MHD-kinetic hybrid code based on structure-preserving finite elements with particles-in-cell

Florian Holderied^{1,2,*}, Stefan Possanner^{1,3}, and Xin Wang¹

¹Max Planck Institute for Plasma Physics, Boltzmannstrasse 2, 85748 Garching, Germany

²Technical University of Munich, Department of Physics, James-Franck-Strasse 1, 85748 Garching, Germany

³Technical University of Munich, Department of Mathematics, Boltzmannstrasse 3, 85748 Garching, Germany

*Corresponding author: Florian Holderied, florian.holderied@ipp.mpg.de

Abstract

We present a STRUCTure-Preserving HYbrid code (STRUPHY) for the simulation of shear-Alfvén waves interacting with a small population of energetic particles far from thermal equilibrium (kinetic species). The code can be run either with current coupling or pressure coupling schemes; it features linearized magneto-hydrodynamic (MHD) equations, coupled nonlinearly to either full-orbit Vlasov or drift-kinetic Vlasov equations. The algorithm is based on finite element exterior calculus (FEEC) for the MHD part and particle-in-cell (PIC) methods for the kinetic part, implemented for arbitrary Riemannian metric in three space dimensions. Noise-reduction via a control variate is optional for the PIC part (δf in contrast to full- f). In the full- f version without control variate, STRUPHY is structure-preserving in the sense that it preserves the discrete energy, zero-divergence constraint and helicity up to machine precision, independent of metric and mesh parameters. Several numerical tests are presented that demonstrate this behavior.

1 Introduction

Plasma waves in magneto-hydrodynamic (MHD) fluids can be resonantly excited by energetic particles with thermal speeds in the range of the Alfvén velocity. Such wave-particle interactions are observed for instance in deuterium-tritium fusion reactors, where hot α -particles can destabilize shear Alfvén modes and thus compromise confinement time [12, 15, 8]. Another example is the interaction of fast electrons in solar wind with Earth's magnetosphere [], frequency chirping need explanations ... []. The associated nonlinear dynamics in realistic scenarios such as fusion reactors or solar wind can be studied via computer simulation of suitable model equations. The latter range from full kinetic models of all involved plasma species (bulk and energetic particles), over hybrid codes to reduced fluid simulations, all compared in a recent benchmark study [13]. The notion of a "hybrid code" implies the following two crucial features:

1. Use of reduced model equations for bulk plasma (for instance fluid instead of kinetic).
2. Fully self-consistent description of nonlinear dynamics (beyond the linear phase).

Examples of successful implementations of hybrid codes are MEGA [21], M3D-K [4, 18], HMGC [5] and HMGC-X [23]. The appeal of hybrid codes is three-fold: a) reduced numerical cost compared to fully kinetic simulations, b) inclusion of non-equilibrium dynamics (wave-particle resonances) compared to pure fluid simulations and c) possibility of direct comparison with analytic computations (for linear dynamics). The drawback is the increased complexity of model equations. For instance, while the geometric structure (ie. Poisson bracket and/or variational principle) of MHD equations has been known for decades [17], the underlying structure of MHD-kinetic hybrid models has been discovered

only very recently [22, 6]. This shows that the proper derivation of MHD-kinetic hybrids that respect fundamental physics principles such as energy conservation is a non-trivial task. As a consequence, little attention had been paid to these issues during the design of the first generation of hybrid codes mentioned above.

In parallel to the theoretical discoveries on how to construct proper hybrid models came the advent of geometric (or structure-preserving) methods for plasma equations, see [16] for a review. These obey many of the conservation properties implied by the geometric structure on the discrete level, such as energy, charge or momentum. The main idea is to discretize directly the underlying Poisson structure or variational principle, thus transferring geometric properties to a finite-dimensional setting. The very first structure-preserving geometric PIC algorithm was designed and implemented by Squire et al. in 2012 [20]. Similar methods have later been successfully applied to Vlasov-Maxwell[10, 19, 26, 25], Vlasov-Darwin [7] and Vlasov-Poisson equations [9, 24]. The first structure-preserving geometric PIC algorithm using finite element exterior calculus (FEEC) was designed by He et al. in 2016 [11]. The same approach has later been taken by Kraus et al. [14] who used B-spline basis functions to efficiently build the discrete deRham complex, which contains Nédélec and Raviart-Thomas spaces. The theoretical foundation of FEEC has been laid by Arnold et al. [3, 1]; the interested reader may consult the recent book of Arnold [2] for a comprehensive overview.

In this work we apply the ideas of structure-preserving integration to MHD-kinetic hybrid models, namely the Hamiltonian current-coupling (CC) and pressure coupling (PC) schemes [22], respectively. In the version of the code presented here, we linearize the MHD part and focus on the nonlinear coupling to the kinetic species, which acts back on the bulk plasma via charge and current densities (CC), or via the pressure tensor (PC). FEEC is used for the discretization of the MHD part in three space dimensions and PIC for the kinetic part. We discretize the equations rather than the variational principle or the Poisson bracket, in order to avoid unnecessary abstraction. Moreover, the linearized MHD equations might lose their Hamiltonian structure if the magnetic background field is not chosen properly. In this case there is no such thing as a Poisson bracket or variational formulation, but our method of discretization still applies. In the semi-discrete setting with continuous time variable, we arrive at a non-canonical Hamiltonian system of ordinary differential equations with skew-symmetric Poisson matrix¹, which directly implies conservation of energy. The conservation of zero-divergence and helicity follow from the proper choice of FEEC spaces (Nédélec and Raviart-Thomas). The conservation laws are satisfied independent of the chosen metric and mesh parameters thanks to the separation between topological and metric properties in the theory of differential forms, upon which FEEC is built. We then use Poisson splitting and show that the described conservation laws translate to the fully discrete setting.

The article is organized as follows: In Sec. 2, we present the model equations which are considered in this work and discuss some of its properties on the continuous level. Sec. 3 is devoted to the discretization of the model in three-dimensional space for arbitrary Riemannian metrics followed by an discussion of some properties of the resulting semi-discrete system of ordinary differential equations with continuous time variable. In Sec. 4, we introduce our time integration scheme based on Poisson splitting. Various numerical results are shown in Sec. 5 before we summarize and conclude in Sec. 6.

¹We cannot prove the Jacobi identity of the Poisson matrix, but speak of a Hamiltonian system anyway to guide ideas.

2 Full model and model reduction

We consider a hybrid kinetic-MHD model where the coupling of the fluid and kinetic species is done via a current coupling scheme. In classical vector calculus notation the model reads

$$\frac{\partial \rho}{\partial t} + \nabla \cdot (\rho \mathbf{U}) = 0, \quad (2.1)$$

$$\frac{\partial \mathbf{U}}{\partial t} + (\mathbf{U} \cdot \nabla) \mathbf{U} = \frac{1}{\rho} (\nabla \times \mathbf{B} + \rho_h \mathbf{U} - \mathbf{j}_h) \times \mathbf{B} - \frac{\nabla p}{\rho}, \quad (2.2)$$

$$\frac{\partial \mathbf{B}}{\partial t} = \nabla \times (\mathbf{U} \times \mathbf{B}), \quad (2.3)$$

$$\frac{\partial p}{\partial t} + \nabla \cdot (p \mathbf{U}) + (\gamma - 1)p \nabla \cdot \mathbf{U} = 0, \quad (2.4)$$

$$\frac{\partial f_h}{\partial t} + \mathbf{v} \cdot \nabla f_h + (\mathbf{B} \times \mathbf{U} + \mathbf{v} \times \mathbf{B}) \cdot \nabla_{\mathbf{v}} f_h = 0, \quad (2.5)$$

$$\rho_h = \int f_h d^3 v, \quad \mathbf{j}_h = \int \mathbf{v} f_h d^3 v. \quad (2.6)$$

where we set all physical constants equal to one². This set of equations forms a closed system of nonlinear partial differential equations for the bulk mass density ρ , the bulk velocity \mathbf{U} , the magnetic induction \mathbf{B} (which we will simply refer to as magnetic field), the bulk pressure p and the distribution function of the hot ions f_h . Furthermore, $\gamma = 5/3$ is the adiabatic exponent. This system possesses a Hamiltonian structure with the following conserved energy:

$$\mathcal{H}_0(t) = \frac{1}{2} \int \rho \mathbf{U}^2 d^3 x + \frac{1}{\gamma - 1} \int p d^3 x + \frac{1}{2} \int \mathbf{B}^2 d^3 x + \frac{1}{2} \int \int \mathbf{v}^2 f_h d^3 v d^3 x. \quad (2.7)$$

In order to start from a simpler model we shall restrict ourselves for the moment on linearized MHD equations by assuming that MHD waves are small perturbations about an equilibrium state. However, we keep all nonlinearities which are related to the coupling to the kinetic species. Making the ansatzes $\mathbf{B} = \mathbf{B}_{\text{eq}} + \tilde{\mathbf{B}}$, $\mathbf{U} = \tilde{\mathbf{U}}$ (zero-flow equilibrium), $\rho = \rho_{\text{eq}} + \tilde{\rho}$ and $p = p_{\text{eq}} + \tilde{p}$ and neglecting nonlinear terms in the MHD part yields

$$\frac{\partial \tilde{\rho}}{\partial t} + \nabla \cdot (\rho_{\text{eq}} \tilde{\mathbf{U}}) = 0, \quad (2.8)$$

$$\rho_{\text{eq}} \frac{\partial \tilde{\mathbf{U}}}{\partial t} = (\nabla \times \tilde{\mathbf{B}}) \times \mathbf{B}_{\text{eq}} + (\nabla \times \mathbf{B}_{\text{eq}}) \times \tilde{\mathbf{B}} + (\rho_h \tilde{\mathbf{U}} - \mathbf{j}_h) \times \mathbf{B} - \nabla \tilde{p}, \quad (2.9)$$

$$\frac{\partial \tilde{\mathbf{B}}}{\partial t} = \nabla \times (\tilde{\mathbf{U}} \times \mathbf{B}_{\text{eq}}), \quad (2.10)$$

$$\frac{\partial \tilde{p}}{\partial t} + \nabla \cdot (p_{\text{eq}} \tilde{\mathbf{U}}) + (\gamma - 1)p_{\text{eq}} \nabla \cdot \tilde{\mathbf{U}} = 0, \quad (2.11)$$

$$\frac{\partial f_h}{\partial t} + \mathbf{v} \cdot \nabla f_h + (\mathbf{B} \times \tilde{\mathbf{U}} + \mathbf{v} \times \mathbf{B}) \cdot \nabla_{\mathbf{v}} f_h = 0. \quad (2.12)$$

The linearization of the MHD part has the consequence that the Hamiltonian (2.7) is no longer conserved. However, if we define the new Hamiltonian

$$\mathcal{H}_1(t) = \frac{1}{2} \int \rho_{\text{eq}} \tilde{\mathbf{U}}^2 d^3 x + \frac{1}{2} \int \tilde{\mathbf{B}}^2 d^3 x + \frac{1}{2} \int \int \mathbf{v}^2 f_h d^3 v d^3 x + \frac{1}{\gamma - 1} \int \tilde{p} d^3 x, \quad (2.13)$$

we get the following energy balance:

$$\frac{d\mathcal{H}_1}{dt} = \int \tilde{\mathbf{U}} \cdot [(\nabla \times \mathbf{B}_{\text{eq}}) \times \tilde{\mathbf{B}}] d^3 x - \int \tilde{\mathbf{U}} \cdot \nabla \tilde{p} d^3 x - \int p_{\text{eq}} \nabla \cdot \tilde{\mathbf{U}} d^3 x \quad (2.14)$$

$$= \int \tilde{\mathbf{U}} \cdot [(\nabla \times \mathbf{B}_{\text{eq}}) \times \tilde{\mathbf{B}}] d^3 x - \int \tilde{\mathbf{U}} \cdot \nabla \tilde{p} d^3 x + \int \tilde{\mathbf{U}} \cdot \nabla p_{\text{eq}} d^3 x. \quad (2.15)$$

We shall use classical particle-in-cell techniques for solving the kinetic equation (2.12) and the frame-

²We assume hot ions with a positive charge. Therefore, one does not have to be careful with the signs in (2.6)

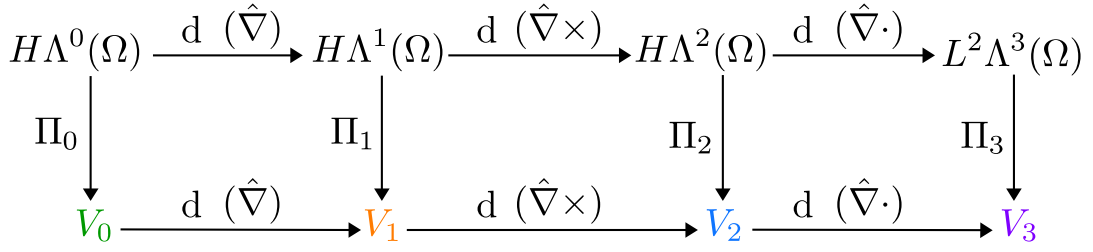


Figure 1: Commuting diagram for function spaces in 3d. The upper line represents the de Rham sequence for the continuous spaces, while the lower line represents the discrete counterpart.

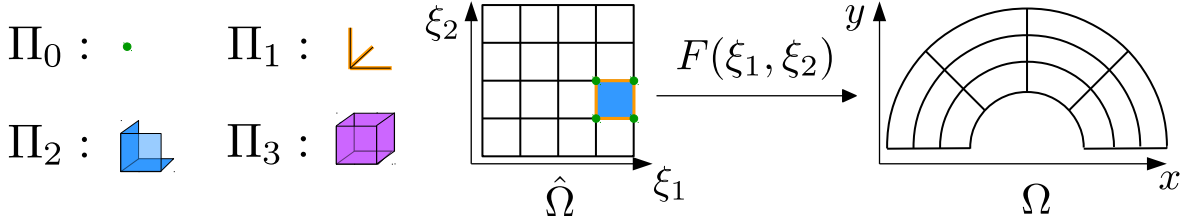


Figure 2: Commuting projectors. Unlike classical finite element methods, the degrees of freedom do not only represent point values, but also edge integrals, face integrals and volume integrals.

work of *finite element exterior calculus* (FEEC) for solving field equations. In the latter, one works with differential forms rather than vector and scalar field. This allows us to treat arbitrary geometries in a natural fashion. For physical reasons we assume the bulk mass density and the hot charge density to be 3-forms ($\rho, \rho_h \rightarrow \rho_{\text{eq}}^3, \rho_h^3$), the magnetic field and the hot ion current density to be 2-forms ($\mathbf{B}, \mathbf{j}_h \rightarrow B^2, j_h^2$) and the pressure to be a 0-form ($p \rightarrow p^0$). The bulk velocity field, which is naturally a vector field, we choose to be a 1-form ($\tilde{\mathbf{U}} \rightarrow \tilde{U}^1$). Eq. (2.8)-(2.11) can then be written as

$$\frac{\partial \tilde{\rho}^3}{\partial t} + \mathrm{d}(i_{\#U^1} \rho_{\text{eq}}^3) = 0, \quad (2.16)$$

$$(*\rho_{\text{eq}}^3) \wedge \frac{\partial \tilde{U}^1}{\partial t} = i_{\diamond B_{\text{eq}}^2} \mathrm{d} * \tilde{B}^2 + i_{\diamond \tilde{B}^2} \mathrm{d} * B_{\text{eq}}^2 - (*\rho_h^3) \wedge i_{\# \tilde{U}^1} B^2 + i_{\diamond j_h^2} B^2 - d \tilde{p}^0, \quad (2.17)$$

$$\frac{\partial \tilde{B}^2}{\partial t} + \mathrm{d}(i_{\#U^1} B_{\text{eq}}^2) = 0, \quad (2.18)$$

$$\frac{\partial \tilde{p}^0}{\partial t} + * \mathrm{d} * (p_{\text{eq}}^0 \wedge U^1) + (\gamma - 1) p_{\text{eq}}^0 \wedge (* \mathrm{d} * U^1) = 0, \quad (2.19)$$

where $*$ is the Hodge-star operator, \wedge the wedge product, i the interior product, $\#$ the sharp operator which transforms a 1-form to a vector field and \diamond the operator which transforms a 2-form to a vector field.

3 Semi-discretization in space

As a next step, we introduce finite element basis functions which satisfy a discrete deRham sequence and which form a commuting diagram with the continuous functions via the interpolation-histopolation projectors Π_0, Π_1, Π_2 and Π_3 . This is depicted in Fig. 1. Assuming that we know the basis functions in each space (how this can be done with e.g. tensor-product B-splines, see Sec. ...), we express the

forms in their respective bases as

$$\tilde{p}^0(t, \boldsymbol{\eta}) \approx \tilde{p}_h^0(t, \boldsymbol{\eta}) = \sum_{\mathbf{i}} p_{\mathbf{i}}(t) \Lambda_{\mathbf{i}}^0(\boldsymbol{\eta}), \quad \mathbf{p}^\top := (p_0(t), \dots, p_{N-1}(t)) \in \mathbb{R}^N, \quad (3.1)$$

$$\tilde{U}^1(t, \boldsymbol{\eta}) \approx \tilde{U}_h^1(t, \boldsymbol{\eta}) = \sum_{\mathbf{i}} \sum_{\mu=1}^3 u_{\mu, \mathbf{i}}(t) \Lambda_{\mu, \mathbf{i}}^1(\boldsymbol{\eta}) d\eta^\mu \quad \mathbf{u}^\top := (\mathbf{u}_1^\top(t), \mathbf{u}_2^\top(t), \mathbf{u}_3^\top(t)) \in \mathbb{R}^{3N}, \quad (3.2)$$

$$\tilde{B}^2(t, \boldsymbol{\eta}) \approx \tilde{B}_h^2(t, \boldsymbol{\eta}) = \sum_{\mathbf{i}} \sum_{\mu=1}^3 b_{\mu, \mathbf{i}}(t) \Lambda_{\mu, \mathbf{i}}^2(\boldsymbol{\eta}) (d\eta^\alpha \wedge d\eta^\beta)_\mu, \quad \mathbf{b}^\top := (\mathbf{b}_1^\top(t), \mathbf{b}_2^\top(t), \mathbf{b}_3^\top(t)) \in \mathbb{R}^{3N}, \quad (3.3)$$

$$\tilde{\rho}^3(t, \boldsymbol{\eta}) \approx \tilde{\rho}_h^3(t, \boldsymbol{\eta}) = \sum_{\mathbf{i}} \rho_{\mathbf{i}}(t) \Lambda_{\mathbf{i}}^3(\boldsymbol{\eta}) d\eta^1 \wedge d\eta^2 \wedge d\eta^3, \quad \boldsymbol{\rho}^\top := (\rho_0(t), \dots, \rho_{N-1}(t)) \in \mathbb{R}^N, \quad (3.4)$$

where $\mathbf{i} = (i_1, i_2, i_3)$ is a multi-index representing the three coordinate directions on the logical domain and $N = N_1 N_2 N_3$ is the total number of basis functions. To simplify the notation, we write for the components of the differential forms

$$\tilde{p}_h^0 \leftrightarrow \tilde{p}_h = (p_0, \dots, p_{N-1}) \begin{pmatrix} \Lambda_0^0 \\ \vdots \\ \Lambda_{N-1}^0 \end{pmatrix} = \mathbf{p}^\top \boldsymbol{\Lambda}^0, \quad \boldsymbol{\Lambda}^0 \in \mathbb{R}^N \quad (3.5)$$

$$\tilde{U}_h^1 \leftrightarrow \tilde{\mathbf{U}}_h^\top = (\mathbf{u}_1^\top, \mathbf{u}_2^\top, \mathbf{u}_3^\top) \begin{pmatrix} \boldsymbol{\Lambda}_1^1 & 0 & 0 \\ 0 & \boldsymbol{\Lambda}_2^1 & 0 \\ 0 & 0 & \boldsymbol{\Lambda}_3^1 \end{pmatrix} = \mathbf{u}^\top \boldsymbol{\Lambda}^1, \quad \boldsymbol{\Lambda}^1 \in \mathbb{R}^{3N \times 3}, \quad (3.6)$$

$$\tilde{B}_h^2 \leftrightarrow \tilde{\mathbf{B}}_h^\top = (\mathbf{b}_1^\top, \mathbf{b}_2^\top, \mathbf{b}_3^\top) \begin{pmatrix} \boldsymbol{\Lambda}_1^2 & 0 & 0 \\ 0 & \boldsymbol{\Lambda}_2^2 & 0 \\ 0 & 0 & \boldsymbol{\Lambda}_3^2 \end{pmatrix} = \mathbf{b}^\top \boldsymbol{\Lambda}^2, \quad \boldsymbol{\Lambda}^2 \in \mathbb{R}^{3N \times 3}, \quad (3.7)$$

$$\tilde{\rho}_h^3 \leftrightarrow \tilde{\rho}_{123,h} = (\rho_0, \dots, \rho_{N-1}) \begin{pmatrix} \Lambda_0^3 \\ \vdots \\ \Lambda_{N-1}^3 \end{pmatrix} = \boldsymbol{\rho}^\top \boldsymbol{\Lambda}^3, \quad \boldsymbol{\Lambda}^3 \in \mathbb{R}^N \quad (3.8)$$

As already stated, we solve the kinetic equation with particle-in-cell techniques. Hence we assume a particle-like distribution function which, in physical space, takes the form

$$f_h = f_h(t, \mathbf{x}, \mathbf{v}) \approx \sum_k w_k(t) \delta(\mathbf{x} - \mathbf{x}_k(t)) \delta(\mathbf{v} - \mathbf{v}_k(t)). \quad (3.9)$$

From this, the hot ion charge density, current density and energy density can easily be obtained by taking the first three moments in velocity space:

$$\dot{\rho}_{h,123}(t, \mathbf{x}) = \sum_k w_k(t) \delta(\mathbf{x} - \mathbf{x}_k(t)), \quad (3.10)$$

$$\dot{\mathbf{j}}_h(t, \mathbf{x}) = \sum_k w_k(t) \delta(\mathbf{x} - \mathbf{x}_k(t)) \mathbf{v}_k(t), \quad (3.11)$$

$$\dot{\epsilon}_{h,123}(t, \mathbf{x}) = \frac{1}{2} \sum_k w_k(t) \delta(\mathbf{x} - \mathbf{x}_k(t)) \mathbf{v}_k^2(t). \quad (3.12)$$

To avoid confusions, we use the notation (\cdot) , where necessary, for quantities which are defined on the physical space. Since there is no difference between vectors/scalars and forms in physical space, these expressions are as well the components of the 3-form number density, the 2-form current density and the 3-form energy density. To get the components on the logical domain we apply the transformation

formulas for 3-forms, respectively 1-forms to obtain

$$\rho_{h,123}(t, \boldsymbol{\eta}) = \sqrt{g} \dot{\rho}_h(t, F(\boldsymbol{\eta})) = \sum_k w_k(t) \delta(\boldsymbol{\eta} - \boldsymbol{\eta}_k(t)), \quad (3.13)$$

$$\mathbf{j}_h(t, \boldsymbol{\eta}) = \sqrt{g} DF^{-1} \dot{\mathbf{j}}_h(t, F(\boldsymbol{\eta})) = DF^{-1} \sum_k w_k(t) \delta(\boldsymbol{\eta} - \boldsymbol{\eta}_k(t)) \mathbf{v}_k(t), \quad (3.14)$$

$$\epsilon_{h,123}(t, \boldsymbol{\eta}) = \sqrt{g} \dot{\epsilon}_h(t, F(\boldsymbol{\eta})) = \frac{1}{2} \sum_k w_k(t) \delta(\boldsymbol{\eta} - \boldsymbol{\eta}_k(t)) \mathbf{v}_k^2(t), \quad (3.15)$$

where we made use of the transformation formula

$$\delta(\mathbf{x} - \mathbf{x}_k(t)) = \frac{1}{\sqrt{g}} \delta(\boldsymbol{\eta} - \boldsymbol{\eta}_k(t)). \quad (3.16)$$

Let us use these results to derive an energy conserving semi-discrete system for the finite element coefficients of \tilde{p}_h^0 , \tilde{U}_h^1 , \tilde{B}_h^2 and $\tilde{\rho}_h^3$ and the particle's positions $(\boldsymbol{\eta}_k)_{k=1,\dots,N_p}$ and velocities $(\mathbf{v}_k)_{k=1,\dots,N_p}$.

3.1 Continuity equation

We start with the discretization of the mass continuity equation which we shall keep in strong form. Following the diagram in Fig. 1, we apply the projector Π_3 and use the diagram's commutativity to exchange projectors and exterior derivatives:

$$\frac{\partial(\Pi_3 \tilde{\rho}^3)}{\partial t} + \Pi_3 d(i_{\# \tilde{U}^1} \rho_{eq}^3) = \frac{\partial \tilde{\rho}_h^3}{\partial t} + d\Pi_2(i_{\# \tilde{U}^1} \rho_{eq}^3) = 0. \quad (3.17)$$

In terms of the components of the forms³, this amounts to

$$\frac{\partial \tilde{\rho}_h}{\partial t} + \hat{\nabla} \cdot \Pi_2 \left[\rho_{eq,123} G^{-1} \tilde{\mathbf{U}}_h \right] = 0, \quad (3.18)$$

$$\Leftrightarrow \frac{\partial \tilde{\rho}_h}{\partial t} + \hat{\nabla} \cdot \Pi_2 \left[\rho_{eq,123} G^{-1} (\Lambda^1)^\top \right] \mathbf{u} = 0, \quad (3.19)$$

$$\Leftrightarrow \frac{d\boldsymbol{\rho}}{dt} + \mathbb{D}\mathcal{Q}\mathbf{u} = 0, \quad (3.20)$$

where we have introduced the discrete divergence matrix $\mathbb{D} \in \mathbb{R}^{N \times 3N}$ and the projection matrix $\mathcal{Q} \in \mathbb{R}^{3N \times 3N}$. We shall use calligraphic symbols for tensors which are related to projections. Explicitly, we have

$$\mathcal{Q}_{ij} := \hat{\Pi}_{2,\mu}^{i_\mu} \left[\rho_{eq,123} G^{\mu k} \Lambda_{jk}^1 \right], \quad i = \begin{cases} i_\mu, & \mu = 1 \\ N + i_\mu, & \mu = 2 \\ 2N + i_\mu, & \mu = 3 \end{cases} \quad (3.21)$$

for $\mu = \{1, 2, 3\}$ and $\hat{\Pi}_{2,\mu}^{i_\mu}$ selects the i_μ -th coefficient of the projection on the space V_2 ($0 \leq i_\mu \leq N-1$). If we stack these coefficients in a column vector, \mathcal{Q} can be written as

$$\mathcal{Q} = \begin{pmatrix} \hat{\Pi}_{2,1} \left[\rho_{eq,123} G^{11} (\Lambda_1^1)^\top \right] & \hat{\Pi}_{2,1} \left[\rho_{eq,123} G^{12} (\Lambda_2^1)^\top \right] & \hat{\Pi}_{2,1} \left[\rho_{eq,123} G^{13} (\Lambda_3^1)^\top \right] \\ \hat{\Pi}_{2,2} \left[\rho_{eq,123} G^{21} (\Lambda_1^1)^\top \right] & \hat{\Pi}_{2,2} \left[\rho_{eq,123} G^{22} (\Lambda_2^1)^\top \right] & \hat{\Pi}_{2,2} \left[\rho_{eq,123} G^{23} (\Lambda_3^1)^\top \right] \\ \hat{\Pi}_{2,3} \left[\rho_{eq,123} G^{31} (\Lambda_1^1)^\top \right] & \hat{\Pi}_{2,3} \left[\rho_{eq,123} G^{32} (\Lambda_2^1)^\top \right] & \hat{\Pi}_{2,3} \left[\rho_{eq,123} G^{33} (\Lambda_3^1)^\top \right] \end{pmatrix} \quad (3.22)$$

$$= \begin{pmatrix} \mathbf{c}_{11,0} & \cdots & \mathbf{c}_{11,N-1} & \mathbf{c}_{12,0} & \cdots & \mathbf{c}_{12,N-1} & \mathbf{c}_{13,0} & \cdots & \mathbf{c}_{13,N-1} \\ \mathbf{c}_{21,0} & \cdots & \mathbf{c}_{21,N-1} & \mathbf{c}_{22,0} & \cdots & \mathbf{c}_{22,N-1} & \mathbf{c}_{23,0} & \cdots & \mathbf{c}_{23,N-1} \\ \mathbf{c}_{31,0} & \cdots & \mathbf{c}_{31,N-1} & \mathbf{c}_{32,0} & \cdots & \mathbf{c}_{32,N-1} & \mathbf{c}_{33,0} & \cdots & \mathbf{c}_{33,N-1} \end{pmatrix}. \quad (3.23)$$

³We use the same symbol for the projectors if it returns the entire form or just its components.

Here, e.g. $\mathbf{c}_{23,0}$ are the coefficients resulting from the projection of the basis function with the index 0 in the block 23 in the matrix (3.22). Unfortunately, this is a dense matrix, which is problematic from a memory consumption point of view. Therefore, we just save the right-hand sides, which define a sparse matrix, and perform the final projection in every time step again. Denoting by $(\mathcal{I}_{2,1}, \mathcal{I}_{2,2}, \mathcal{I}_{2,3})$ the mixed interpolation-histopolation matrices and by $(\text{vec}_{2,1}(f^2), \text{vec}_{2,2}(f^2), \text{vec}_{2,3}(f^2))$ the right-hand side vectors for a 2-form f^2 , we can write

$$Q = \begin{pmatrix} \mathcal{I}_{2,1}^{-1} & 0 & 0 \\ 0 & \mathcal{I}_{2,2}^{-1} & 0 \\ 0 & 0 & \mathcal{I}_{2,3}^{-1} \end{pmatrix} \begin{pmatrix} \text{vec}_{2,1}^{11}(\mathcal{Q}) & \text{vec}_{2,1}^{12}(\mathcal{Q}) & \text{vec}_{2,1}^{13}(\mathcal{Q}) \\ \text{vec}_{2,1}^{21}(\mathcal{Q}) & \text{vec}_{2,1}^{22}(\mathcal{Q}) & \text{vec}_{2,1}^{23}(\mathcal{Q}) \\ \text{vec}_{2,1}^{31}(\mathcal{Q}) & \text{vec}_{2,1}^{32}(\mathcal{Q}) & \text{vec}_{2,1}^{33}(\mathcal{Q}) \end{pmatrix} =: \mathcal{I}_2^{-1} \tilde{\mathcal{Q}}. \quad (3.24)$$

Thus, we only precompute the matrices $\tilde{\mathcal{Q}}$ and \mathcal{I}_2 , whose sparsity immediately from the local support of the basis functions.

3.2 Momentum equation

We choose a weak formulation for the momentum equation. Consequently, we take the inner product with a test function $C^1 \in H\Lambda^1(\Omega)$ to obtain the variational formulation: Find $\tilde{U}^1 \in H\Lambda^1(\Omega)$ such that

$$\left((*\rho_{\text{eq}}^3) \wedge \frac{\partial \tilde{U}^1}{\partial t}, C^1 \right) = \left(i_{\diamond B_{\text{eq}}^2} d * \tilde{B}^2, C^1 \right) + \left(i_{\diamond \tilde{B}^2} d * B_{\text{eq}}^2, C^1 \right) - \left(d \tilde{p}^0, C^1 \right) \quad (3.25)$$

$$- \left((*\rho_h^3) \wedge i_{\# \tilde{U}^2} B^2, C^1 \right) + \left(i_{\diamond j_h^2} B^2, C^1 \right) \quad \forall C^1 \in H\Lambda^1(\Omega). \quad (3.26)$$

We apply the Galerkin approximation to each term and project back into the right spaces where necessary. Let us start with the first term on the left-hand side involving the equilibrium bulk density. To achieve conservation of energy at the discrete level we make use of the fact that the wedge product with a 0-form is just a multiplication with a scalar. Hence the wedge product can as well be applied to the test function and the following equality holds:

$$\left((*\rho_{\text{eq}}^3) \wedge \frac{\partial \tilde{U}^1}{\partial t}, C^1 \right) = \frac{1}{2} \left((*\rho_{\text{eq}}^3) \wedge \frac{\partial \tilde{U}^1}{\partial t}, C^1 \right) + \frac{1}{2} \left(\frac{\partial \tilde{U}^1}{\partial t}, (*\rho_{\text{eq}}^3) \wedge C^1 \right). \quad (3.27)$$

Using the definition of the inner product of 1-forms involving the metric tensor G^{-1} yields for the first term

$$\left((*\rho_{\text{eq}}^3) \wedge \frac{\partial \tilde{U}^1}{\partial t}, C^1 \right) = \int_{\hat{\Omega}} \frac{1}{\sqrt{g}} \rho_{\text{eq},123} \left(\frac{\partial \tilde{\mathbf{U}}}{\partial t} \right)^T G^{-1} \mathbf{C} \sqrt{g} d^3\eta \quad (3.28)$$

$$\approx \int_{\hat{\Omega}} \Pi_1 \left[\frac{1}{\sqrt{g}} \rho_{\text{eq},123} \left(\frac{\partial \tilde{\mathbf{U}}_h}{\partial t} \right)^T \right] G^{-1} \mathbf{C}_h \sqrt{g} d^3\eta \quad (3.29)$$

$$= \dot{\mathbf{u}}^T \mathcal{W}^T \underbrace{\int_{\hat{\Omega}} \mathbb{A}^1 G^{-1} (\mathbb{A}^1)^T \sqrt{g} d^3\eta}_{=: \mathbb{M}^1} \mathbf{c} = \dot{\mathbf{u}}^T \mathcal{W}^T \mathbb{M}^1 \mathbf{c} \quad \forall \mathbf{c} \in \mathbb{R}^{3N}, \quad (3.30)$$

where $\mathbb{M}^1 \in \mathbb{R}^{3N \times 3N}$ is the mass matrix in the space V_1 and the projection matrix is given by

$$\mathcal{W}_{ij} = \hat{\Pi}_{1,\mu}^{i_\mu} \left[\frac{\rho_{\text{eq},123}}{\sqrt{g}} \Lambda_{j\mu}^1 \right]. \quad (3.31)$$

Finally, we obtain

$$\left((*\rho_{\text{eq}}^3) \wedge \frac{\partial \tilde{U}^1}{\partial t}, C^1 \right) \approx \frac{1}{2} \mathbf{c}^T (\mathbb{M}^1 \mathcal{W} + \mathcal{W}^T \mathbb{M}^1) \dot{\mathbf{u}} =: \mathbf{c}^T \mathcal{A} \dot{\mathbf{u}}, \quad (3.32)$$

with $\mathcal{A} \in \mathbb{R}^{3N \times 3N}$ being symmetric.

For the first term on the right-hand side, we make use of the identities $\langle i_{\diamond} \gamma^2 \alpha^2, \beta^1 \rangle = \langle \alpha^2, * \gamma^2 \wedge \beta^1 \rangle$ and $*(*\alpha^2 \wedge \beta^1) = i_{\# \beta^1} \alpha^2$, such that we obtain

$$(i_{\diamond} B_{\text{eq}}^2 d * \tilde{B}^2, C^1) = (d * \tilde{B}^2, * B_{\text{eq}}^2 \wedge C^1) = (* d * \tilde{B}^2, *(* B_{\text{eq}}^2 \wedge C^1)) = (d^* \tilde{B}^2, i_{\# C^1} B_{\text{eq}}^2), \quad (3.33)$$

where we introduced the co-differential operator $d^* \alpha^p = (-1)^p * d * \alpha^p$. Applying the Green formula for differential forms and assuming that the resulting boundary term vanishes yields

$$(i_{\diamond} B_{\text{eq}}^2 d * \tilde{B}^2, C^1) = (\tilde{B}^2, d i_{\# C^1} B_{\text{eq}}^2) = \int_{\hat{\Omega}} \frac{1}{g} \tilde{\mathbf{B}}^\top G [\hat{\nabla} \times (\mathbf{B}_{\text{eq}} \times G^{-1} \mathbf{C})] \sqrt{g} d^3 \eta \quad (3.34)$$

$$\approx \mathbf{b}^\top \underbrace{\int_{\hat{\Omega}} \frac{1}{\sqrt{g}} \mathbb{A}^2 G (\mathbb{A}^2)^\top d^3 \eta}_{=: \mathbb{M}^2} \mathbb{C} \hat{\Pi}_1 [\mathbb{B}_{\text{eq}} G^{-1} (\mathbb{A}^1)^\top] \mathbf{c} = \mathbf{b}^\top \mathbb{M}^2 \mathbb{C} \mathcal{T} \mathbf{c} \quad \forall \mathbf{c} \in \mathbb{R}^{3N}, \quad (3.35)$$

where we introduced the mass matrix $\mathbb{M}^2 \in \mathbb{R}^{3N \times 3N}$ in the space V_2 and the discrete curl matrix $\mathbb{C} \in \mathbb{R}^{3N \times 3N}$. Moreover, we wrote the vector product of the background magnetic field with the test function in terms of a matrix-vector product by using the anti-symmetric matrix

$$\mathbb{B}_{\text{eq}} := \begin{pmatrix} 0 & -B_{\text{eq},3} & B_{\text{eq},2} \\ B_{\text{eq},3} & 0 & -B_{\text{eq},1} \\ -B_{\text{eq},2} & B_{\text{eq},1} & 0 \end{pmatrix} \in \mathbb{R}^{3 \times 3}. \quad (3.36)$$

The projection matrix \mathcal{T} is given by

$$\mathcal{T}_{ij} := \hat{\Pi}_{1,\mu}^{i_\mu} [\mathbb{B}_{\text{eq},\mu k} G^{kl} \Lambda_{j,l}^1] = \hat{\Pi}_{1,\mu}^{i_\mu} [\epsilon_{\mu m k} B_{\text{eq},m} G^{kl} \Lambda_{j,l}^1], \quad \mu = \{1, 2, 3\}, \quad (3.37)$$

which has the right-hand sides

$$\tilde{\mathcal{T}} = \begin{pmatrix} \text{vec}_{1,1} [(B_{\text{eq},2} G^{31} - B_{\text{eq},3} G^{21})(\Lambda_1^1)^\top, (B_{\text{eq},2} G^{32} - B_{\text{eq},3} G^{22})(\Lambda_2^1)^\top, (B_{\text{eq},2} G^{33} - B_{\text{eq},3} G^{23})(\Lambda_3^1)^\top] \\ \text{vec}_{1,2} [(B_{\text{eq},3} G^{11} - B_{\text{eq},1} G^{31})(\Lambda_1^1)^\top, (B_{\text{eq},3} G^{12} - B_{\text{eq},1} G^{32})(\Lambda_2^1)^\top, (B_{\text{eq},3} G^{13} - B_{\text{eq},1} G^{33})(\Lambda_3^1)^\top] \\ \text{vec}_{1,3} [(B_{\text{eq},1} G^{21} - B_{\text{eq},2} G^{11})(\Lambda_1^1)^\top, (B_{\text{eq},1} G^{22} - B_{\text{eq},2} G^{12})(\Lambda_2^1)^\top, (B_{\text{eq},1} G^{23} - B_{\text{eq},2} G^{13})(\Lambda_3^1)^\top] \end{pmatrix} \quad (3.38)$$

Performing the same steps for the second term without integration by parts yields

$$(i_{\diamond} \tilde{B}^2 d * B_{\text{eq}}^2, C^1) = \int_{\hat{\Omega}} \mathbf{C}^\top G^{-1} \left[\left(\hat{\nabla} \times \frac{1}{\sqrt{g}} G \mathbf{B}_{\text{eq}} \right) \times \frac{1}{\sqrt{g}} \tilde{\mathbf{B}} \right] \sqrt{g} d^3 \eta \quad (3.39)$$

$$\approx \mathbf{c}^\top \int_{\hat{\Omega}} \mathbb{A}^1 G^{-1} (\mathbb{A}^1)^\top d^3 \eta \hat{\Pi}_1 \left[\frac{1}{\sqrt{g}} \mathbb{B}_{\text{eq}}^{\nabla \times} (\mathbb{A}^2)^\top \right] \mathbf{b} = \mathbf{c}^\top \mathbb{M}^1 \mathcal{P} \mathbf{b} \quad \forall \mathbf{c} \in \mathbb{R}^{3N}. \quad (3.40)$$

The projection matrix $\mathcal{P} \in \mathbb{R}^{3N \times 3N}$ is given by

$$\mathcal{P}_{ij} = \hat{\Pi}_{1,\mu}^{i_\mu} \left[\frac{1}{\sqrt{g}} \mathbb{B}_{\text{eq},\mu k}^{\nabla \times} \Lambda_{kj}^2 \right]. \quad (3.41)$$

As a next step, we consider the term involving the pressure gradient:

$$(d\tilde{p}^0, C^1) = (d\tilde{p}^0, C^1) = \int_{\hat{\Omega}} \hat{\nabla} \tilde{p}^\top G^{-1} \mathbf{C} \sqrt{g} d^3 \eta \quad (3.42)$$

$$\approx \mathbf{p}^\top \mathbb{G}^\top \int_{\hat{\Omega}} \mathbb{A}^1 G^{-1} (\mathbb{A}^1)^\top d^3 \eta \mathbf{c} = \mathbf{p}^\top \mathbb{G}^\top \mathbb{M}^1 \mathbf{c} \quad \forall \mathbf{c} \in \mathbb{R}^{3N}, \quad (3.43)$$

with $\mathbb{G} \in \mathbb{R}^{3N \times N}$ being the discrete gradient matrix. The term involving the hot ion charge density must be computed from the particle-in-cell approximation of the hot ion distribution function. Hence

we can generally make use of a control variate M_0 for variance reduction:

$$\left((*\rho_h^3) \wedge i_{\# \tilde{U}^1} B^2, C^1 \right) = \int_{\hat{\Omega}} \mathbf{C}^\top G^{-1} \left(\rho_h^3 \mathbf{B} \times G^{-1} \tilde{\mathbf{U}} \right) \sqrt{g} d^3 \eta \quad (3.44)$$

$$= \int_{\hat{\Omega}} \mathbf{C}^\top G^{-1} \left[\int (\dot{f}_h^0 - \dot{M}_0) d^3 v \mathbf{B} \times G^{-1} \tilde{\mathbf{U}} \right] \sqrt{g} d^3 \eta + \int_{\hat{\Omega}} \mathbf{C}^\top G^{-1} \left(\int \dot{M}_0 d^3 v \mathbf{B} \times G^{-1} \tilde{\mathbf{U}} \right) \sqrt{g} d^3 \eta \quad (3.45)$$

$$= \int_{\hat{\Omega}} \int \left\{ \mathbf{C}^\top G^{-1} \left[\left(\frac{f_h^0 - M_0}{g_h} \right) \mathbf{B} \times G^{-1} \tilde{\mathbf{U}} \right] \right\} g_h d^3 v d^3 \eta + \int_{\hat{\Omega}} \mathbf{C}^\top \left(\frac{\rho_{h0}}{\sqrt{g}} G \mathbf{B} \times \tilde{\mathbf{U}} \right) d^3 \eta. \quad (3.46)$$

In the last line we introduced the probability density g_h which satisfies the Vlasov equation and which is normalized to one for the first term and we used the identity $G \mathbf{a}_1 \times G \mathbf{a}_2 = g G^{-1} (\mathbf{a}_1 \times \mathbf{a}_2)$ for arbitrary vectors \mathbf{a}_1 and $\mathbf{a}_2 \in \mathbb{R}^3$. This allows us interpret the expression in the curly brackets of the first term as a random variable and we can write down the Monte Carlo estimate

$$\left((*\rho_h^3) \wedge i_{\# \tilde{U}^1} B^2, C^1 \right) \quad (3.47)$$

$$\approx \sum_k \underbrace{\frac{1}{N_k} \left(\frac{f_h^0(\boldsymbol{\eta}_k, \mathbf{v}_k^0)}{g_h^0(\boldsymbol{\eta}_k, \mathbf{v}_k^0)} - \frac{M_0(\boldsymbol{\eta}_k, \mathbf{v}_k)}{g_h^0(\boldsymbol{\eta}_k, \mathbf{v}_k^0)} \right)}_{=: w_k(t)} \mathbf{C}_h^\top(\boldsymbol{\eta}) G^{-1}(\boldsymbol{\eta}_k) (\mathbf{B}_h(\boldsymbol{\eta}_k) \times G^{-1}(\boldsymbol{\eta}_k) \tilde{\mathbf{U}}_h(\boldsymbol{\eta}_k)) \quad (3.48)$$

$$+ \mathbf{c}^\top \int_{\hat{\Omega}} \mathbb{A}^1 \frac{\rho_{h0}}{\sqrt{g}} G \mathbb{B}(\mathbb{A}^1)^\top d^3 \eta \mathbf{u} \quad (3.49)$$

$$= \sum_k w_k \mathbf{C}_h^\top(\boldsymbol{\eta}_k) G^{-1}(\boldsymbol{\eta}_k) (\mathbf{B}_h(\boldsymbol{\eta}_k) \times G^{-1}(\boldsymbol{\eta}_k) \tilde{\mathbf{U}}_h(\boldsymbol{\eta}_k)) + \mathbf{c}^\top \mathbb{X}(\mathbf{b}) \mathbf{u} \quad (3.50)$$

$$= \mathbf{c}^\top \mathbb{P}^1 \mathbb{W} \bar{G}^{-1} \bar{\mathbb{B}} \bar{G}^{-1} \mathbb{P}^{1\top} \mathbf{u} + \mathbf{c}^\top \mathbb{X}(\mathbf{b}) \mathbf{u}, \quad (3.51)$$

where both terms are clearly anti-symmetric because \mathbb{B} is anti-symmetric. In the last line we introduced the anti-symmetric block matrix $\bar{\mathbb{B}} \in \mathbb{R}^{3N_p \times 3N_p}$ given by

$$\bar{\mathbb{B}} = \bar{\mathbb{B}}(\mathbf{b}, \boldsymbol{\eta}) = \begin{pmatrix} 0 & -\text{diag}[\mathbb{P}_3^{2\top}(\boldsymbol{\eta}) \mathbf{b}_3] & \text{diag}[\mathbb{P}_2^{2\top}(\boldsymbol{\eta}) \mathbf{b}_2] \\ \text{diag}[\mathbb{P}_3^{2\top}(\boldsymbol{\eta}) \mathbf{b}_3] & 0 & -\text{diag}[\mathbb{P}_1^{2\top}(\boldsymbol{\eta}) \mathbf{b}_1] \\ -\text{diag}[\mathbb{P}_2^{2\top}(\boldsymbol{\eta}) \mathbf{b}_2] & \text{diag}[\mathbb{P}_1^{2\top}(\boldsymbol{\eta}) \mathbf{b}_1] & 0 \end{pmatrix} + \bar{\mathbb{B}}_{\text{eq}}(\eta), \quad (3.52)$$

where N_p is the number of particles and $\boldsymbol{\eta} \in \mathbb{R}^{3N_p}$ is a vector holding all particle positions. Moreover, we define the following matrices:

- $\mathbb{P}_{\mu, ik}^1 = \Lambda_{\mu, i}^1(\boldsymbol{\eta}_k) \in \mathbb{R}^{N \times N_p}, \quad \mathbb{P}_{\mu, ik}^2 = \Lambda_{\mu, i}^2(\boldsymbol{\eta}_k) \in \mathbb{R}^{N \times N_p},$
- $\mathbb{P}^1 = \text{diag}(\mathbb{P}_1^1, \mathbb{P}_2^1, \mathbb{P}_3^1) \in \mathbb{R}^{3N \times 3N_p}, \quad \mathbb{P}^2 = \text{diag}(\mathbb{P}_1^2, \mathbb{P}_2^2, \mathbb{P}_3^2) \in \mathbb{R}^{3N \times 3N_p}$
- $\mathbb{W} = \mathbb{I}_3 \otimes \text{diag}(w_1, \dots, w_{N_p}) \in \mathbb{R}^{3N_p \times 3N_p},$
- $(\bar{G}^{-1})_{ab} = \text{diag}[(G^{-1})_{ab}(\boldsymbol{\eta})] \quad 1 \leq a, b \leq 3$
- $(D\bar{F}^{-1})_{ab} = \text{diag}[(DF^{-1})_{ab}(\boldsymbol{\eta})] \quad 1 \leq a, b \leq 3$

A similar procedure for the term involving the hot ion current density yields

$$\left(i_{\diamond j_h^2} B^2, C^1 \right) = \int_{\hat{\Omega}} \mathbf{C}^\top G^{-1} \left(\mathbf{B} \times \frac{1}{\sqrt{g}} \mathbf{j}_h \right) \sqrt{g} d^3 \eta \quad (3.53)$$

$$= \int_{\hat{\Omega}} \mathbf{C}^\top G^{-1} \left[\mathbf{B} \times DF^{-1} \int (\dot{f}_h - \dot{M}_0) \mathbf{v} d^3 v \right] \sqrt{g} d^3 \eta \quad (3.54)$$

$$+ \int_{\hat{\Omega}} \mathbf{C}^\top G^{-1} \left[\mathbf{B} \times DF^{-1} \int \dot{M}_0 \mathbf{v} d^3 v \right] \sqrt{g} d^3 \eta \quad (3.55)$$

$$= \int_{\hat{\Omega}} \mathbf{C}^\top G^{-1} \left[\mathbf{B} \times DF^{-1} \left(\frac{f_h - M_0}{g_h} \right) \mathbf{v} \right] g_h d^3 v d^3 \eta + \int_{\hat{\Omega}} \mathbf{C}^\top \left(\frac{1}{\sqrt{g}} G \mathbf{B} \times DF^\top \mathbf{j}_{h0} \right) d^3 \eta \quad (3.56)$$

$$\approx \sum_k w_k \mathbf{C}_h^\top(\boldsymbol{\eta}_k) \bar{G}^{-1}(\boldsymbol{\eta}_k) [\mathbf{B}_h(\boldsymbol{\eta}_k) \times DF^{-1}(\boldsymbol{\eta}_k) \mathbf{v}_k] + \mathbf{c}^\top \int_{\hat{\Omega}} \mathbb{A}^1 \left(\frac{1}{\sqrt{g}} G \mathbf{B}_h \times DF^\top \mathbf{j}_{h0} \right) d^3 \eta \quad (3.57)$$

$$= \mathbf{c}^\top \mathbb{P}^1 \mathbb{W} \bar{G}^{-1} \bar{\mathbb{B}} D\bar{F}^{-1} \mathbf{V} + \mathbf{c}^\top \mathbf{x}(\mathbf{b}) \quad \forall \mathbf{c} \in \mathbb{R}^{3N}. \quad (3.58)$$

Here, $\mathbf{V} = (v_{1x}, \dots, v_{N_p x}, v_{1y}, \dots, v_{N_p y}, v_{1z}, \dots, v_{N_p z}) \in \mathbb{R}^{3N_p}$ is the vector holding all particle velocities. The second term is just the right-hand side of the L^2 -projection in the space V_1 of the function inside the round brackets and can be computed numerically for some given magnetic field. In total we get the following semi-discrete momentum balance equation:

$$\mathcal{A}\dot{\mathbf{u}} = \mathcal{T}^\top \mathbb{C}^\top \mathbb{M}^2 \mathbf{b} + \mathbb{M}^1 \mathcal{P} \mathbf{b} - \mathbb{M}^1 \mathbb{G} \mathbf{p} - \mathbb{P}^1 \mathbb{W} \bar{G}^{-1} \bar{\mathbb{B}} G^{-1} \mathbb{P}^{1\top} \mathbf{u} - \mathbb{X} \mathbf{u} + \mathbb{P}^1 \mathbb{W} \bar{G}^{-1} \bar{\mathbb{B}} D F^{-1} \mathbf{V} + \mathbf{x}. \quad (3.59)$$

Note that recovering the full- f case just means choosing the control variate $\mathcal{M}_0 = 0$ which results in $\mathbb{X} = 0$ and $\mathbf{x} = 0$.

3.3 Induction equation

Like the mass continuity equation, we keep the induction equation in strong form. Hence we apply the projector Π_2 and once more use the diagram's commutativity to exchange projectors and exterior derivatives:

$$\frac{\partial(\Pi_2 \tilde{B}^2)}{\partial t} + \Pi_2 d(i_{\#U^1} B_{\text{eq}}^2) = \frac{\partial(\Pi_2 \tilde{B}^2)}{\partial t} + d\Pi_1(i_{\#U^1} B_{\text{eq}}^2). \quad (3.60)$$

In terms of the components of the forms, this amounts to

$$\frac{\partial \tilde{\mathbf{B}}_h}{\partial t} + \hat{\nabla} \times \Pi_1 \left[\mathbf{B}_{\text{eq}} \times G^{-1} \tilde{\mathbf{U}}_h \right] = 0 \quad (3.61)$$

$$\Leftrightarrow \frac{\partial \tilde{\mathbf{B}}_h}{\partial t} + \hat{\nabla} \times \Pi_1 \left[\mathbb{B}_{\text{eq}} G^{-1} (\mathbb{A}^1)^\top \right] \mathbf{u} = 0 \quad (3.62)$$

$$\Leftrightarrow \frac{d\mathbf{b}}{dt} + \mathbb{C} \mathcal{T} \mathbf{u} = 0. \quad (3.63)$$

We immediately see that we obtain the same projection matrix \mathcal{T} as for the Hall term in the momentum equation.

3.4 Pressure equation

We once more choose a weak formulation for the pressure equation. Hence we take the inner product with a test function $r^0 \in H\Lambda^0(\Omega)$ which yields the variational formulation: find $\tilde{p}^0 \in H\Lambda^0(\Omega)$ such that

$$\left(\frac{\partial \tilde{p}^0}{\partial t}, r^0 \right) - (d^*(p_{\text{eq}}^0 \wedge \tilde{U}^1), r^0) - (\gamma - 1)(d^*\tilde{U}^1, p_{\text{eq}}^0 \wedge r^0) = 0 \quad \forall r^0 \in H\Lambda^0(\Omega) \quad (3.64)$$

$$\Leftrightarrow \left(\frac{\partial \tilde{p}^0}{\partial t}, r^0 \right) - (p_{\text{eq}}^0 \wedge \tilde{U}^1, dr^0) - (\gamma - 1)(\tilde{U}^1, d(p_{\text{eq}}^0 \wedge r^0)) = 0 \quad \forall r^0 \in H\Lambda^0(\Omega), \quad (3.65)$$

if we again assume all boundary terms to vanish. For the first term we simply get

$$\left(\frac{\partial \tilde{p}^0}{\partial t}, r^0 \right) = \int_{\hat{\Omega}} \frac{\partial \tilde{p}}{\partial t} r \sqrt{g} d^3 \eta \approx \dot{\mathbf{p}}^\top \underbrace{\int_{\hat{\Omega}} \mathbf{\Lambda}^0 (\mathbf{\Lambda}^0)^\top \sqrt{g} d^3 \eta \mathbf{r}}_{=: \mathbb{M}^0} \quad (3.66)$$

where $\mathbb{M}^0 \in \mathbb{R}^{N \times N}$ is the mass matrix in the space V_0 . The second term amounts to

$$(p_{\text{eq}}^0 \wedge \tilde{U}^1, dr^0) = \int_{\hat{\Omega}} p_{\text{eq}} \tilde{\mathbf{U}}^\top G^{-1} \hat{\nabla} r \sqrt{g} d^3 \eta \quad (3.67)$$

$$= \mathbf{u}^\top \hat{\Pi}_1 [p_{\text{eq}} \mathbb{A}^1] \int_{\hat{\Omega}} \mathbb{A}^1 G^{-1} (\mathbb{A}^1)^\top \sqrt{g} d^3 \eta \mathbb{G} \mathbf{r} = \mathbf{u}^\top \mathcal{S}^\top \mathbb{M}^1 \mathbb{G} \mathbf{r} \quad \forall \mathbf{r} \in \mathbb{R}^N, \quad (3.68)$$

where the projection matrix $\mathcal{S} \in \mathbb{R}^{3N \times 3N}$ is defined as

$$\mathcal{S}_{ij} := \hat{\Pi}_{1,\mu}^{i_\mu} [p_{\text{eq}} \Lambda_{j\mu}^1]. \quad (3.69)$$

Finally, we obtain for the last term

$$(\tilde{U}^1, d(p_{\text{eq}}^0 \wedge r^0)) = \int_{\hat{\Omega}} \tilde{\mathbf{U}}^\top G^{-1} \hat{\nabla}(p_{\text{eq}} r) \sqrt{g} d^3\eta \quad (3.70)$$

$$= \mathbf{u}^\top \int_{\hat{\Omega}} \mathbb{A}^1 G^{-1} (\mathbb{A}^1)^\top \sqrt{g} d^3\eta \mathbb{G} \hat{\Pi}_0 [p_{\text{eq}} (\Lambda^0)^\top] \mathbf{r} = \mathbf{u}^\top \mathbb{M}^1 \mathbb{G} \mathcal{K} \mathbf{r} \quad \forall \mathbf{r} \in \mathbb{R}^N. \quad (3.71)$$

The new projection matrix $\mathcal{K} \in \mathbb{R}^{N \times N}$ is given by

$$\mathcal{K}_{ij} := \hat{\Pi}_0^i [p_{\text{eq}} \Lambda_j^0]. \quad (3.72)$$

Summing up all terms yields the following semi-discrete pressure equation:

$$\dot{\mathbf{p}}^\top \mathbb{M}^0 \mathbf{r} - \mathbf{u}^\top \mathcal{S}^\top \mathbb{M}^1 \mathbb{G} \mathbf{r} - (\gamma - 1) \mathbf{u}^\top \mathbb{M}^1 \mathbb{G} \mathcal{K} \mathbf{r} = 0 \quad \forall \mathbf{r} \in \mathbb{R}^N \quad (3.73)$$

$$\Leftrightarrow \mathbb{M}^0 \dot{\mathbf{p}} = \mathbb{G}^\top \mathbb{M}^1 \mathcal{S} \mathbf{u} + (\gamma - 1) \mathcal{K}^\top \mathbb{G}^\top \mathbb{M}^1 \mathbf{u}. \quad (3.74)$$

3.5 Particles' equation of motion

As a last step, we derive the equations of motion for a single particle with logical coordinates $\boldsymbol{\eta}_k$ and physical velocity \mathbf{v}_k . For the latter, we have to push-forward the forms B^2 and \tilde{U}^1 to physical space:

$$\frac{d\boldsymbol{\eta}_k}{dt} = DF^{-1}(\boldsymbol{\eta}_k) \mathbf{v}_k, \quad (3.75)$$

$$\frac{d\mathbf{v}_k}{dt} = \frac{1}{\sqrt{g(\boldsymbol{\eta}_k)}} DF(\boldsymbol{\eta}_k) \mathbf{B}_h(\boldsymbol{\eta}_k) \times DF^{-\top}(\boldsymbol{\eta}_k) \tilde{\mathbf{U}}_h(\boldsymbol{\eta}_k) - \frac{1}{\sqrt{g(\boldsymbol{\eta}_k)}} DF(\boldsymbol{\eta}_k) \mathbf{B}_h(\boldsymbol{\eta}_k) \times \mathbf{v}_k. \quad (3.76)$$

$$= DF^{-\top}(\boldsymbol{\eta}_k) [\mathbf{B}_h(\boldsymbol{\eta}_k) \times G^{-1}(\boldsymbol{\eta}_k) \mathbf{U}_h(\boldsymbol{\eta}_k)] - DF^{-\top}(\boldsymbol{\eta}_k) [\mathbf{B}_h(\boldsymbol{\eta}_k) \times DF^{-1}(\boldsymbol{\eta}_k) \mathbf{v}_k], \quad (3.77)$$

where we used once more the identity $A\mathbf{b} \times A\mathbf{c} = \det(A)A^{-\top}(\mathbf{b} \times \mathbf{c})$ from vector calculus. Writing the above equation of motion in matrix-vector form for all particles yields

$$\frac{d\mathbf{H}}{dt} = \bar{DF}^{-1}(\mathbf{H}) \mathbf{V}, \quad (3.78)$$

$$\frac{d\mathbf{V}}{dt} = \bar{DF}^{-\top}(\mathbf{H}) \bar{\mathbb{B}}(\mathbf{b}, \mathbf{H}) \bar{G}^{-1}(\mathbf{H}) \mathbb{P}^{1\top}(\mathbf{H}) \mathbf{u} - \bar{DF}^{-\top}(\mathbf{H}) \bar{\mathbb{B}}(\mathbf{b}, \mathbf{H}) \bar{DF}^{-1}(\mathbf{H}) \mathbf{V}. \quad (3.79)$$

3.6 Hamiltonian system

Let us try to write the semi-discrete system of equation in Hamiltonian form. For this, we define the discrete Hamiltonian

$$\mathcal{H}_h := \frac{1}{2} ((\ast \rho_{\text{eq}}^3) \wedge \tilde{U}_h^1, \tilde{U}_h^1) + \frac{1}{2} (\tilde{B}_h^2, \tilde{B}_h^2) + \frac{1}{\gamma - 1} (\tilde{p}^0, 1) + \frac{1}{2} \int_{\hat{\Omega}} \epsilon_{h,123} d^3\eta \quad (3.80)$$

$$= \frac{1}{2} \mathbf{u}^\top \mathcal{A} \mathbf{u} + \frac{1}{2} \mathbf{b}^\top \mathbb{M}^2 \mathbf{b} + \frac{1}{\gamma - 1} \mathbf{p}^\top \mathbf{n} + \frac{1}{2} \mathbf{V}^\top \mathbb{W}(\mathbf{H}, \mathbf{V}) \mathbf{V} + \epsilon_{h0} := \mathcal{H}_{h1} + \frac{1}{\gamma - 1} \mathbf{p}^\top \mathbf{n} + \epsilon_{h0}. \quad (3.81)$$

With this we can write the semi-discrete system in the following form:

$$\frac{d}{dt} \begin{pmatrix} \rho \\ \mathbf{u} \\ \mathbf{b} \\ \mathbf{p} \\ \mathbf{H} \\ \mathbf{V} \end{pmatrix} = \begin{pmatrix} 0 & 0 & 0 & 0 & 0 \\ 0 & \mathbb{J}_{11}(\mathbf{b}, \mathbf{H}, \mathbf{V}) & \mathbb{J}_{12} & 0 & \mathbb{J}_{14}(\mathbf{b}, \mathbf{H}) \\ 0 & -\mathbb{J}_{12}^\top & 0 & 0 & 0 \\ 0 & 0 & 0 & 0 & 0 \\ 0 & 0 & 0 & 0 & \mathbb{J}_{34}(\mathbf{H}, \mathbf{V}) \\ 0 & -\mathbb{J}_{14}^\top(\mathbf{b}, \mathbf{H}) & 0 & 0 & -\mathbb{J}_{34}^\top(\mathbf{H}, \mathbf{V}) + \mathbb{J}_{44}(\mathbf{b}, \mathbf{H}, \mathbf{V}) \end{pmatrix} \begin{pmatrix} 0 \\ \mathcal{A}\mathbf{u} \\ \mathbb{M}^2\mathbf{b} \\ 0 \\ 0 \\ \mathbb{W}(\mathbf{H}, \mathbf{V})\mathbf{V} \end{pmatrix} \quad (3.82)$$

$$+ \begin{pmatrix} 0 & -\mathbb{D}\mathcal{Q} & 0 & 0 & 0 & 0 \\ 0 & -\mathcal{A}^{-1}\mathbb{X}(\mathbf{b}) & \mathcal{A}^{-1}\mathbb{M}^1\mathcal{P} & -\mathcal{A}^{-1}\mathbb{M}^1\mathbb{G} & 0 & 0 \\ 0 & 0 & 0 & 0 & 0 & 0 \\ 0 & (\mathbb{M}^0)^{-1}\mathbb{G}^\top\mathbb{M}^1\mathcal{S} + (\gamma - 1)(\mathbb{M}^0)^{-1}\mathcal{K}^\top\mathbb{G}^\top\mathbb{M}^1 & 0 & 0 & 0 & 0 \\ 0 & 0 & 0 & 0 & 0 & 0 \\ 0 & 0 & 0 & 0 & 0 & 0 \end{pmatrix} \begin{pmatrix} \rho \\ \mathbf{u} \\ \mathbf{b} \\ \mathbf{p} \\ \mathbf{H} \\ \mathbf{V} \end{pmatrix} \quad (3.83)$$

$$+ \begin{pmatrix} 0 \\ \mathcal{A}^{-1}\mathbf{x}(\mathbf{b}) \\ 0 \\ 0 \\ 0 \\ 0 \end{pmatrix}. \quad (3.84)$$

We see that we can write the system as the sum of a non-canonical Hamiltonian part (first matrix-vector product) with the Hamiltonian \mathcal{H}_{h1} and additional non-Hamiltonian parts. The latter vanishes if we you use the full- f description (then \mathbb{X} and \mathbf{x} vanish), if $\nabla \times \mathbf{B}_{\text{eq}} = 0$ (then $\mathcal{P} = 0$) and if there are no pressure and density perturbations. The blocks in the Poisson matrix of the Hamiltonian part are given by

$$\mathbb{J}_{11}(\mathbf{b}, \mathbf{H}, \mathbf{V}) = -\mathcal{A}^{-1}\mathbb{P}^1(\mathbf{H})\mathbb{W}(\mathbf{H}, \mathbf{V})\bar{\mathcal{G}}^{-1}(\mathbf{H})\bar{\mathcal{B}}(\mathbf{b}, \mathbf{H})\bar{\mathcal{G}}^{-1}(\mathbf{H})\mathbb{P}^{1\top}(\mathbf{H})\mathcal{A}^{-1}, \quad (3.85)$$

$$\mathbb{J}_{12} = \mathcal{A}^{-1}\mathcal{T}^\top\mathbb{C}^\top, \quad (3.86)$$

$$\mathbb{J}_{14}(\mathbf{b}, \mathbf{H}) = \mathcal{A}^{-1}\mathbb{P}^1(\mathbf{H})\tilde{\mathcal{G}}^{-1}(\mathbf{H})\bar{\mathcal{B}}(\mathbf{b}, \mathbf{H})\tilde{\mathcal{D}}F^{-1}(\mathbf{H}), \quad (3.87)$$

$$\mathbb{J}_{34}(\mathbf{H}, \mathbf{V}) = \tilde{\mathcal{D}}F^{-1}(\mathbf{H})\mathbb{W}^{-1}(\mathbf{H}, \mathbf{V}), \quad (3.88)$$

$$\mathbb{J}_{44}(\mathbf{b}, \mathbf{H}, \mathbf{V}) = -\tilde{\mathcal{D}}F^{-\top}(\mathbf{H})\bar{\mathcal{B}}(\mathbf{b}, \mathbf{H})\tilde{\mathcal{D}}F^{-1}(\mathbf{H})\mathbb{W}^{-1}(\mathbf{H}, \mathbf{V}). \quad (3.89)$$

We now turn our attention to the integration of this system in time.

4 Time integration

4.1 Poisson splitting for Hamiltonian part

We split the Poisson matrix into antisymmetric sub-systems such that each sub-system again defines a Hamiltonian system

$$\frac{d}{dt} \begin{pmatrix} \mathbf{u} \\ \mathbf{b} \\ \mathbf{Q} \\ \mathbf{V} \end{pmatrix} = \begin{pmatrix} \mathbb{J}_{11}(\mathbf{b}, \mathbf{Q}) & \mathbb{J}_{12} & 0 & \mathbb{J}_{14}(\mathbf{b}, \mathbf{Q}) \\ -\mathbb{J}_{12}^\top & 0 & 0 & 0 \\ 0 & 0 & 0 & \mathbb{J}_{34}(\mathbf{Q}) \\ -\mathbb{J}_{14}^\top(\mathbf{b}, \mathbf{Q}) & 0 & -\mathbb{J}_{34}^\top(\mathbf{Q}) & \mathbb{J}_{44}(\mathbf{b}, \mathbf{Q}) \end{pmatrix} \begin{pmatrix} \mathcal{A}\mathbf{u} \\ \mathbb{M}^2\mathbf{b} \\ 0 \\ \mathbb{W}\mathbf{V} \end{pmatrix}, \quad (4.1)$$

$$\mathbb{J}_{11}(\mathbf{b}, \mathbf{Q}) = -\mathcal{A}^{-1}\mathbb{P}_1(\mathbf{Q})\mathbb{W}\tilde{G}^{-1}(\mathbf{Q})\hat{\mathbb{B}}(\mathbf{b}, \mathbf{Q})\tilde{G}^{-1}(\mathbf{Q})\mathbb{P}_1^\top(\mathbf{Q})\mathcal{A}^{-1}, \quad (4.2)$$

$$\mathbb{J}_{12} = \mathcal{A}^{-1}\mathcal{T}^\top\mathbb{C}^\top, \quad (4.3)$$

$$\mathbb{J}_{14}(\mathbf{b}, \mathbf{Q}) = \mathcal{A}^{-1}\mathbb{P}_1(\mathbf{Q})\tilde{G}^{-1}(\mathbf{Q})\hat{\mathbb{B}}(\mathbf{b}, \mathbf{Q})\tilde{D}F^{-1}(\mathbf{Q}), \quad (4.4)$$

$$\mathbb{J}_{34}(\mathbf{Q}) = \tilde{D}F^{-1}(\mathbf{Q})\mathbb{W}^{-1}, \quad (4.5)$$

$$\mathbb{J}_{44}(\mathbf{Q}) = -\tilde{D}F^{-\top}(\mathbf{Q})\hat{\mathbb{B}}(\mathbf{b}, \mathbf{Q})\tilde{D}F^{-1}(\mathbf{Q})\mathbb{W}^{-1}. \quad (4.6)$$

Sub-step 1 The first sub-system reads

$$\dot{\mathbf{u}} = \mathbb{J}_{11}(\mathbf{b}, \mathbf{Q})\mathcal{A}\mathbf{u}, \quad (4.7)$$

$$\dot{\mathbf{b}} = 0, \quad (4.8)$$

$$\dot{\mathbf{Q}} = 0, \quad (4.9)$$

$$\dot{\mathbf{V}} = 0. \quad (4.10)$$

We solve this equation with the energy-preserving Crank-Nicolson method:

$$\frac{\mathbf{u}^{n+1} - \mathbf{u}^n}{\Delta t} = \mathbb{J}_{11}(\mathbf{b}^n, \mathbf{Q}^n)\mathcal{A}\frac{\mathbf{u}^n + \mathbf{u}^{n+1}}{2}. \quad (4.11)$$

$$\Leftrightarrow \left(\mathbb{I} - \frac{\Delta t}{2}\mathbb{J}_{11}(\mathbf{b}^n, \mathbf{Q}^n)\mathcal{A} \right) \mathbf{u}^{n+1} = \left(\mathbb{I} + \frac{\Delta t}{2}\mathbb{J}_{11}(\mathbf{b}^n, \mathbf{Q}^n)\mathcal{A} \right) \mathbf{u}^n. \quad (4.12)$$

To avoid multiple matrix inversions, we multiply everything with \mathcal{A} from the left to obtain

$$\left(\mathcal{A} - \frac{\Delta t}{2}\mathcal{A}\mathbb{J}_{11}(\mathbf{b}^n, \mathbf{Q}^n)\mathcal{A} \right) \mathbf{u}^{n+1} = \left(\mathcal{A} + \frac{\Delta t}{2}\mathcal{A}\mathbb{J}_{11}(\mathbf{b}^n, \mathbf{Q}^n)\mathcal{A} \right) \mathbf{u}^n. \quad (4.13)$$

We denote the corresponding integrator by $\Phi_{\Delta t}^1$.

Sub-step 2 The second sub-system reads

$$\dot{\mathbf{u}} = \mathbb{J}_{12}\mathbb{M}^2\mathbf{b}, \quad (4.14)$$

$$\dot{\mathbf{b}} = -\mathbb{J}_{12}^\top\mathcal{A}\mathbf{u}, \quad (4.15)$$

$$\dot{\mathbf{Q}} = 0, \quad (4.16)$$

$$\dot{\mathbf{V}} = 0. \quad (4.17)$$

We again solve this system with an energy-preserving Crank-Nicolson method:

$$\begin{pmatrix} \mathcal{A} & -\frac{\Delta t}{2}\mathcal{T}^\top\mathbb{C}^\top\mathbb{M}^2 \\ \frac{\Delta t}{2}\mathbb{C}\mathcal{T} & \mathbb{I} \end{pmatrix} \begin{pmatrix} \mathbf{u}^{n+1} \\ \mathbf{b}^{n+1} \end{pmatrix} = \begin{pmatrix} \mathcal{A} & \frac{\Delta t}{2}\mathcal{T}^\top\mathbb{C}^\top\mathbb{M}^2 \\ -\frac{\Delta t}{2}\mathbb{C}\mathcal{T} & \mathbb{I} \end{pmatrix} \begin{pmatrix} \mathbf{u}^n \\ \mathbf{b}^n \end{pmatrix}. \quad (4.18)$$

Using the Schur complement $S := \mathcal{A} + \frac{\Delta t^2}{4} \mathcal{T}^\top \mathbb{C}^\top \mathbb{M}^2 \mathbb{C} \mathcal{T}$, we can calculate the inverse of the matrix on the left-hand side which we can then multiply with the matrix on the right-hand side:

$$\begin{pmatrix} \mathcal{S}^{-1} & \frac{\Delta t}{2} \mathcal{S}^{-1} \mathcal{T}^\top \mathbb{C}^\top \mathbb{M}^2 \\ -\frac{\Delta t}{2} \mathbb{C} \mathcal{T} \mathcal{S}^{-1} & \mathbb{I} - \frac{\Delta t^2}{4} \mathbb{C} \mathcal{T} \mathcal{S}^{-1} \mathcal{T}^\top \mathbb{C}^\top \mathbb{M}^2 \end{pmatrix} \begin{pmatrix} \mathcal{A} & \frac{\Delta t}{2} \mathcal{T}^\top \mathbb{C}^\top \mathbb{M}^2 \\ -\frac{\Delta t}{2} \mathbb{C} \mathcal{T} & \mathbb{I} \end{pmatrix} = \quad (4.19)$$

$$= \begin{pmatrix} \mathcal{S}^{-1} \mathcal{A} - \frac{\Delta t^2}{4} \mathcal{S}^{-1} \mathcal{T}^\top \mathbb{C}^\top \mathbb{M}^2 \mathbb{C} \mathcal{T} & \Delta t \mathcal{S}^{-1} \mathcal{T}^\top \mathbb{C}^\top \mathbb{M}^2 \\ -\frac{\Delta t}{2} \mathbb{C} \mathcal{T} \mathcal{S}^{-1} \mathcal{A} - \frac{\Delta t}{2} \mathbb{C} \mathcal{T} + \frac{\Delta t^3}{8} \mathbb{C} \mathcal{T} \mathcal{S}^{-1} \mathcal{T}^\top \mathbb{C}^\top \mathbb{M}^2 \mathbb{C} \mathcal{T} & \mathbb{I} - \frac{\Delta t^2}{2} \mathbb{C} \mathcal{T} \mathcal{S}^{-1} \mathcal{T}^\top \mathbb{C}^\top \mathbb{M}^2 \end{pmatrix} \quad (4.20)$$

$$\Rightarrow \mathbf{u}^{n+1} = \mathcal{S}^{-1} \left[\left(\mathcal{A} - \frac{\Delta t^2}{4} \mathcal{T}^\top \mathbb{C}^\top \mathbb{M}^2 \mathbb{C} \mathcal{T} \right) \mathbf{u}^n + \Delta t \mathcal{T}^\top \mathbb{C}^\top \mathbb{M}^2 \mathbf{b}^n \right] \quad (4.21)$$

$$\Rightarrow \mathbf{b}^{n+1} = \mathbf{b}^n - \frac{\Delta t}{2} \mathbb{C} \mathcal{T} \left(\mathbf{u}^n + \mathcal{S}^{-1} \mathcal{A} \mathbf{u}^n - \frac{\Delta t^2}{2} \mathcal{S}^{-1} \mathcal{T}^\top \mathbb{C}^\top \mathbb{M}^2 \mathbb{C} \mathcal{T} \mathbf{u}^n + \Delta t \mathcal{S}^{-1} \mathcal{T}^\top \mathbb{C}^\top \mathbb{M}^2 \mathbf{b}^n \right) \quad (4.22)$$

$$= \mathbf{b}^n - \frac{\Delta t}{2} \mathbb{C} \mathcal{T} (\mathbf{u}^n + \mathbf{u}^{n+1}) \quad (4.23)$$

We immediately see that the update for \mathbf{b} preserves the divergence-free constraint. We denote the corresponding integrator by $\Phi_{\Delta t}^2$.

Sub-step 3 The third sub-system reads

$$\dot{\mathbf{u}} = \mathbb{J}_{14}(\mathbf{b}, \mathbf{Q}) \mathbb{W} \mathbf{V}, \quad (4.24)$$

$$\dot{\mathbf{b}} = 0, \quad (4.25)$$

$$\dot{\mathbf{Q}} = 0, \quad (4.26)$$

$$\dot{\mathbf{V}} = -\mathbb{J}_{14}^\top(\mathbf{b}, \mathbf{Q}) \mathcal{A} \mathbf{u}. \quad (4.27)$$

We solve this system in the same way as before. Since \mathbf{b} and \mathbf{Q} do not change in this step, the same is true for the matrix \mathbb{J}_{14} . Hence $\mathbb{J}_{14} = \mathbb{J}_{14}(\mathbf{b}^n, \mathbf{Q}^n)$ and we have

$$\begin{pmatrix} \mathcal{A} & -\frac{\Delta t}{2} \mathcal{A} \mathbb{J}_{14} \mathbb{W} \\ \frac{\Delta t}{2} \mathbb{J}_{14}^\top \mathcal{A} & \mathbb{I} \end{pmatrix} \begin{pmatrix} \mathbf{u}^{n+1} \\ \mathbf{V}^{n+1} \end{pmatrix} = \begin{pmatrix} \mathcal{A} & \frac{\Delta t}{2} \mathcal{A} \mathbb{J}_{14} \mathbb{W} \\ -\frac{\Delta t}{2} \mathbb{J}_{14}^\top \mathcal{A} & \mathbb{I} \end{pmatrix} \begin{pmatrix} \mathbf{u}^n \\ \mathbf{V}^n \end{pmatrix}. \quad (4.28)$$

Using once more the Schur complement $\mathcal{S}^{-1} := \mathcal{A} + \frac{\Delta t^2}{4} \mathcal{A} \mathbb{J}_{14} \mathbb{W} \mathbb{J}_{14}^\top \mathcal{A}$ yields

$$\mathbf{u}^{n+1} = \mathcal{S}^{-1} \left[\left(\mathcal{A} - \frac{\Delta t^2}{4} \mathcal{A} \mathbb{J}_{14} \mathbb{W} \mathbb{J}_{14}^\top \mathcal{A} \right) \mathbf{u}^n + \Delta t \mathcal{A} \mathbb{J}_{14} \mathbb{W} \mathbf{V}^n \right], \quad (4.29)$$

$$\mathbf{V}^{n+1} = \mathbf{V}^n - \frac{\Delta t}{2} \mathbb{J}_{14}^\top \mathcal{A} (\mathbf{u}^n + \mathbf{u}^{n+1}) \quad (4.30)$$

We denote the corresponding integrator by $\Phi_{\Delta t}^3$.

Sub-step 4 The fourth sub-system reads

$$\dot{\mathbf{u}} = 0, \quad (4.31)$$

$$\dot{\mathbf{b}} = 0, \quad (4.32)$$

$$\dot{\mathbf{Q}} = \mathbb{J}_{34}(\mathbf{Q}) \mathbb{W} \mathbf{V}, \quad (4.33)$$

$$\dot{\mathbf{V}} = 0. \quad (4.34)$$

Using again a Crank-Nicolson approximation for particle k yields

$$\mathbf{q}_k^{n+1} = \mathbf{q}_k^n + \frac{\Delta t}{2} (DF^{-1}(\mathbf{q}_k^n) + DF^{-1}(\mathbf{q}_k^{n+1})) \mathbf{v}_k^n, \quad (4.35)$$

which can be solved for \mathbf{q}^{n+1} using a fix point iteration. We denote the corresponding integrator by $\Phi_{\Delta t}^4$.

Sub-step 5 The fifth sub-system reads

$$\dot{\mathbf{u}} = 0, \quad (4.36)$$

$$\dot{\mathbf{b}} = 0, \quad (4.37)$$

$$\dot{\mathbf{Q}} = 0, \quad (4.38)$$

$$\dot{\mathbf{V}} = \mathbb{J}_{44}(\mathbf{b}, \mathbf{Q})\mathbb{W}\mathbf{V}. \quad (4.39)$$

Using again a Crank-Nicolson approximation for particle k yields

$$\left(\mathbb{I} + \frac{\Delta t}{2} DF^{-\top}(\mathbf{q}_k^n) \hat{\mathbb{B}}_h(\mathbf{q}_k^n) DF^{-1}(\mathbf{q}_k^n) \right) \mathbf{v}_k^{n+1} = \left(\mathbb{I} - \frac{\Delta t}{2} DF^{-\top}(\mathbf{q}_k^n) \hat{\mathbb{B}}_h(\mathbf{q}_k^n) DF^{-1}(\mathbf{q}_k^n) \right) \mathbf{v}_k^n. \quad (4.40)$$

We denote the corresponding integrator by $\Phi_{\Delta t}^5$.

5 Dispersion relation

In this section we derive the dispersion relation for wave propagation parallel to an external, uniform magnetic field $\mathbf{B} = B_0 \mathbf{e}_z$. Although we have $\mathbf{E} = -\mathbf{U} \times \mathbf{B}$ in ideal MHD, we assume for the moment a general electric field. With this, linearization of the Vlasov equation about an homogeneous (in space) equilibrium $f_h^0 = f_h^0(v_\parallel, v_\perp)$ yields

$$\frac{\partial f_h}{\partial t} + \mathbf{v} \cdot \nabla f_h + \Omega_{\text{ch}}(\mathbf{v} \times \mathbf{e}_z) \cdot \nabla_{\mathbf{v}} f_h = -\frac{q_h}{m_h} (\mathbf{E} + \mathbf{v} \times \mathbf{B}) \cdot \nabla_{\mathbf{v}} f_h^0. \quad (5.1)$$

The solution of this equation in Fourier space leads to an Ohm's law of the form

$$\hat{\mathbf{j}}_h = \begin{pmatrix} -i \frac{q_h^2}{m_h} \int \frac{v_\perp(\omega - kv_\parallel)}{2\Omega_+ \Omega_-} \hat{G} f_h^0 d^3 v & \frac{q_h^2}{m_h} \Omega_{\text{ch}} \int \frac{v_\perp}{2\Omega_+ \Omega_-} \hat{G} f_h^0 d^3 v & 0 \\ -i \frac{q_h^2}{m_h} \Omega_{\text{ch}} \int \frac{v_\perp}{2\Omega_+ \Omega_-} \hat{G} f_h^0 d^3 v & -i \frac{q_h^2}{m_h} \int \frac{v_\perp(\omega - kv_\parallel)}{2\Omega_+ \Omega_-} \hat{G} f_h^0 d^3 v & 0 \\ 0 & 0 & -i \frac{q_h^2}{m_h} \int \frac{v_\parallel}{\omega - kv_\parallel} \partial_\parallel f_h^0 d^3 v \end{pmatrix} \hat{\mathbf{E}} = \sigma_h(k, \omega) \hat{\mathbf{E}}, \quad (5.2)$$

where $\hat{G} = \partial/\partial v_\perp + k(v_\perp \partial/\partial v_\parallel - v_\parallel \partial/\partial v_\perp)/\omega$ is a differential operator measuring the anisotropy of the distribution function and velocity space and $\Omega_\pm = \omega - kv_\parallel \pm \Omega_{\text{ce}}$ denote the frequencies of resonant particles. We make now use of the fact that $\hat{\mathbf{E}} = -B_0 \hat{\mathbf{U}} \times \mathbf{e}_z$ in ideal MHD. This yields a pure transverse current with components

$$\hat{j}_{hx} = -\sigma_{hxx} B_0 U_y + \sigma_{hxy} B_0 U_x \quad (5.3)$$

$$\hat{j}_{hy} = -\sigma_{hyx} B_0 U_y + \sigma_{hyy} B_0 U_x. \quad (5.4)$$

The momentum balance equation then reads

$$-i\omega \hat{\mathbf{U}} + i \frac{v_A^2 k^2}{\omega} \hat{\mathbf{U}}_\perp + i \frac{c_S^2 k^2}{\omega} \mathbf{e}_z \hat{U}_\parallel = \frac{Z_h \nu_h \Omega_{\text{ch}}}{A_{\text{MHD}}} \hat{\mathbf{U}} \times \mathbf{e}_z + \frac{B_0}{\rho_{\text{eq}}} (\mathbf{e}_z \times \hat{\mathbf{j}}_h), \quad (5.5)$$

where we approximated the bulk mass density by the ion contribution $\rho_{\text{eq}} = A_{\text{MHD}} m_i n_0$, Z_h is the hot ion charge number and $\nu_h = n_{h0}/n_0$ is the ratio of the equilibrium bulk and energetic ion number densities. Writing everything in terms of the bulk velocity yields the linear system

$$\begin{pmatrix} \omega^2 - v_A^2 k^2 + iv_A^2 \sigma_{hyy} \omega & i \left(-\frac{Z_h \nu_h \Omega_{\text{ch}} \omega}{A_{\text{MHD}}} - v_A^2 \sigma_{hyx} \omega \right) & 0 \\ -i \left(-\frac{Z_h \nu_h \Omega_{\text{ch}} \omega}{A_{\text{MHD}}} + v_A^2 \sigma_{hxy} \omega \right) & \omega^2 - v_A^2 k^2 + iv_A^2 \sigma_{hxx} \omega & 0 \\ 0 & 0 & \omega^2 - c_S^2 k^2 \end{pmatrix} \begin{pmatrix} \hat{U}_x \\ \hat{U}_y \\ \hat{U}_\parallel \end{pmatrix} = 0. \quad (5.6)$$

The structure of this system immediately reveals that we deal with circularly polarized waves in perpendicular direction characterized by $iU_x/U_y = \pm 1$ for R/L-waves, respectively. This leads to the dispersion relation

$$D_{R/L}(k, \omega) = 1 - \frac{v_A^2 k^2}{\omega^2} + \frac{iv_A^2 \sigma_{hxx}}{\omega} \pm \frac{Z_h \nu_h \Omega_{ch}}{A_{MHD}\omega} \mp \frac{v_A^2 \sigma_{hxy}}{\omega} \quad (5.7)$$

$$= 1 - \frac{v_A^2 k^2}{\omega^2} \pm \frac{Z_h \nu_h \Omega_{ch}}{A_{MHD}\omega} + \frac{\nu_h \Omega_{ch}^2 Z_h^2}{A_h A_{MHD}\omega} \int \frac{v_\perp}{2} \frac{\hat{G}F_h^0}{\omega - kv_\parallel \pm \Omega_{ch}} d^3 v = 0. \quad (5.8)$$

Assuming a shifted, isotropic Maxwellian of the form

$$F_h^0 = \frac{1}{\pi^{3/2} v_{th}^3} \exp \left(-\frac{(v_\parallel - v_0)^2 + v_\perp^2}{v_{th}^2} \right) \quad (5.9)$$

$$\Rightarrow \frac{\partial F_h^0}{\partial v_\parallel} = -F_h^0 \frac{2}{v_{th}^2} (v_\parallel - v_0) \quad (5.10)$$

$$\Rightarrow \frac{\partial F_h^0}{\partial v_\perp} = -F_h^0 \frac{2}{v_{th}^2} v_\perp \quad (5.11)$$

$$\Rightarrow \hat{G}F_h^0 = -F_h^0 \frac{2}{v_{th}^2} v_\perp + \frac{k}{\omega} F_h^0 \frac{2}{v_{th}^2} v_\perp v_0 = F_h^0 \frac{2v_\perp}{v_{th}^2} \left(\frac{kv_0}{\omega} - 1 \right) \quad (5.12)$$

$$\Rightarrow \pi \int_0^\infty \frac{1}{\pi^{3/2} v_{th}^3} \begin{pmatrix} 1 \\ v_\perp \\ v_\perp^2 \\ v_\perp^3 \end{pmatrix} \exp \left(-\frac{v_\perp^2}{v_{th}^2} \right) dv_\perp = \begin{pmatrix} 1/(2v_{th}^2) \\ 1/(2v_{th}\sqrt{\pi}) \\ 1/4 \\ v_{th}/(2\sqrt{\pi}) \end{pmatrix}, \quad (5.13)$$

leads to

$$D_{R/L}(k, \omega) = 1 - \frac{v_A^2 k^2}{\omega^2} \pm \frac{Z_h \nu_h \Omega_{ch}}{A_{MHD}\omega} + \frac{\nu_h \Omega_{ch}^2 Z_h^2}{A_h A_{MHD}\omega^2} \frac{\omega - kv_0}{kv_{th}} Z(\eta^\pm), \quad (5.14)$$

where Z is the plasma dispersion function and $\eta^\pm = (\omega - kv_0 \pm \Omega_{ch})/(kv_{th})$.

References

- [1] D. Arnold, R. Falk, and R. Winther. Finite element exterior calculus: from Hodge theory to numerical stability. *Bulletin of the American mathematical society*, 47(2):281–354, 2010.
- [2] D. N. Arnold. *Finite element exterior calculus*, volume 93. SIAM, 2018.
- [3] D. N. Arnold, R. S. Falk, and R. Winther. Finite element exterior calculus, homological techniques, and applications. *Acta numerica*, 15:1–155, 2006.
- [4] E. Belova, R. Denton, and A. Chan. Hybrid simulations of the effects of energetic particles on low-frequency MHD waves. *Journal of Computational Physics*, 136(2):324–336, 1997.
- [5] S. Briguglio, G. Vlad, F. Zonca, and C. Kar. Hybrid magnetohydrodynamic-gyrokinetic simulation of toroidal Alfvén modes. *Physics of Plasmas*, 2(10):3711–3723, 1995.
- [6] J. W. Burby and C. Tronci. Variational approach to low-frequency kinetic-MHD in the current coupling scheme. *Plasma Physics and Controlled Fusion*, 59(4):045013, 2017.
- [7] G. Chen and L. Chacón. An energy-and charge-conserving, nonlinearly implicit, electromagnetic 1D-3V Vlasov–Darwin particle-in-cell algorithm. *Computer Physics Communications*, 185(10):2391–2402, 2014.
- [8] L. Chen and F. Zonca. Physics of Alfvén waves and energetic particles in burning plasmas. *Reviews of Modern Physics*, 88(1):015008, 2016.

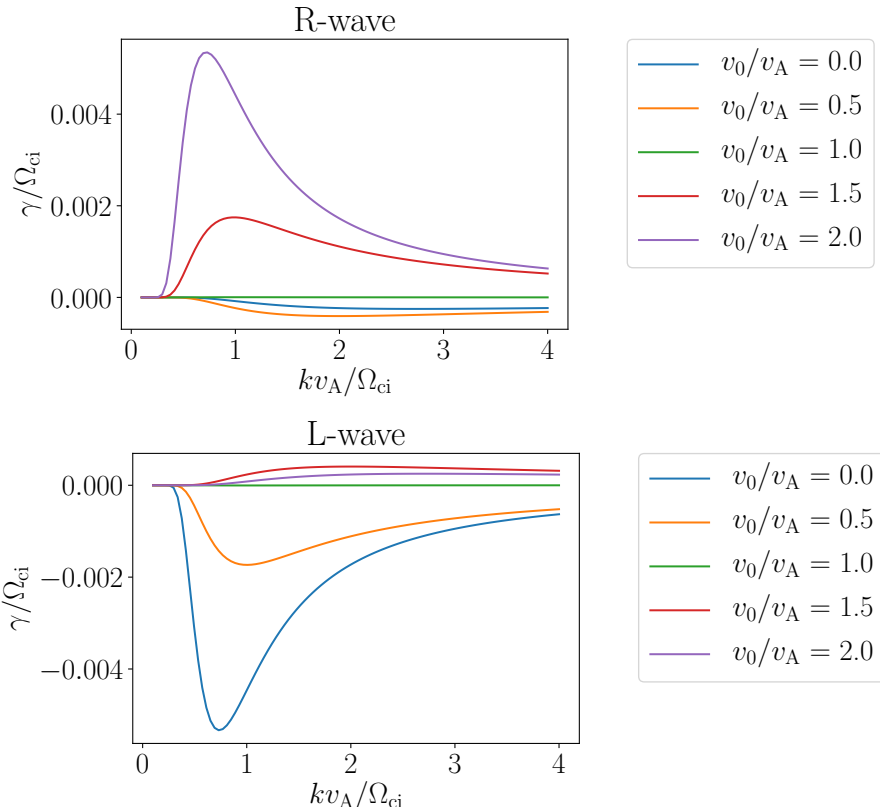


Figure 3: Growth rates for different shifts of the Maxwellian

- [9] E. Evstatiev and B. Shadwick. Variational formulation of particle algorithms for kinetic plasma simulations. *Journal of Computational Physics*, 245:376–398, 2013.
- [10] Y. He, H. Qin, Y. Sun, J. Xiao, R. Zhang, and J. Liu. Hamiltonian time integrators for Vlasov-Maxwell equations. *Physics of Plasmas*, 22(12):124503, 2015.
- [11] Y. He, Y. Sun, H. Qin, and J. Liu. Hamiltonian particle-in-cell methods for Vlasov-Maxwell equations. *Physics of Plasmas*, 23(9):092108, 2016.
- [12] W. Heidbrink. Basic physics of Alfvén instabilities driven by energetic particles in toroidally confined plasmas. *Physics of Plasmas*, 15(5):055501, 2008.
- [13] A. Könies, S. Briguglio, N. Gorelenkov, T. Fehér, M. Isaev, P. Lauber, A. Mishchenko, D. Spong, Y. Todo, W. Cooper, et al. Benchmark of gyrokinetic, kinetic MHD and gyrofluid codes for the linear calculation of fast particle driven TAE dynamics. *Nuclear Fusion*, 58(12):126027, 2018.
- [14] M. Kraus, K. Kormann, P. J. Morrison, and E. Sonnendrücker. GEMPIC: Geometric electromagnetic particle-in-cell methods. *Journal of Plasma Physics*, 83(4), 2017.
- [15] P. Lauber. Super-thermal particles in hot plasmas—Kinetic models, numerical solution strategies, and comparison to tokamak experiments. *Physics Reports*, 533(2):33–68, 2013.
- [16] P. J. Morrison. Structure and structure-preserving algorithms for plasma physics. *Physics of Plasmas*, 24(5):055502, 2017.
- [17] P. J. Morrison and J. M. Greene. Noncanonical Hamiltonian density formulation of hydrodynamics and ideal magnetohydrodynamics. *Physical Review Letters*, 45(10):790, 1980.
- [18] W. Park, E. Belova, G. Fu, X. Tang, H. Strauss, and L. Sugiyama. Plasma simulation studies using multilevel physics models. *Physics of Plasmas*, 6(5):1796–1803, 1999.

- [19] H. Qin, J. Liu, J. Xiao, R. Zhang, Y. He, Y. Wang, Y. Sun, J. W. Burby, L. Ellison, and Y. Zhou. Canonical symplectic particle-in-cell method for long-term large-scale simulations of the Vlasov–Maxwell equations. *Nuclear Fusion*, 56(1):014001, 2015.
- [20] J. Squire, H. Qin, and W. M. Tang. Geometric integration of the Vlasov-Maxwell system with a variational particle-in-cell scheme. *Physics of Plasmas*, 19(8):084501, 2012.
- [21] Y. Todo and T. Sato. Linear and nonlinear particle-magnetohydrodynamic simulations of the toroidal Alfvén eigenmode. *Physics of plasmas*, 5(5):1321–1327, 1998.
- [22] C. Tronci. Hamiltonian approach to hybrid plasma models. *Journal of Physics A: Mathematical and Theoretical*, 43(37):375501, 2010.
- [23] X. Wang, S. Briguglio, L. Chen, C. Di Troia, G. Fogaccia, G. Vlad, and F. Zonca. An extended hybrid magnetohydrodynamics gyrokinetic model for numerical simulation of shear Alfvén waves in burning plasmas. *Physics of Plasmas*, 18(5):052504, 2011.
- [24] J. Xiao and H. Qin. Field theory and a structure-preserving geometric particle-in-cell algorithm for drift wave instability and turbulence. *Nuclear Fusion*, 59(10):106044, 2019.
- [25] J. XIAO, H. QIN, and J. LIU. Structure-preserving geometric particle-in-cell methods for Vlasov–Maxwell systems. *Plasma Science and Technology*, 20(11):110501, sep 2018.
- [26] J. Xiao, H. Qin, J. Liu, and R. Zhang. Local energy conservation law for a spatially-discretized Hamiltonian Vlasov-Maxwell system. *Physics of Plasmas*, 24(6):062112, 2017.